

---

# ADVERSARIAL REPRESENTATION LEARNING FOR SYNTHETIC REPLACEMENT OF PRIVATE ATTRIBUTES

**John Martinsson** **Edvin Listo Zec** **Daniel Gillblad** **Olof Mogren**  
RISE Research Institutes of Sweden  
john.martinsson@ri.se

## ABSTRACT

Data privacy is an increasingly important aspect of the analysis of big data for many real-world tasks. Privacy enhancing transformations of data can help unlocking the potential in data sources containing sensitive information, but finding the right balance between privacy and utility is often a tricky trade-off. In this work, we study how adversarial representation learning can be used to ensure the privacy of users, and to obfuscate sensitive attributes in existing datasets. While previous methods using this kind of approach only aim at obfuscating the sensitive information, we find that adding new information in its place strengthens the provided privacy. We propose a two step data privatization method that builds on generative adversarial networks: in the first step, sensitive data is removed from the representation, and in the second step, a sample which is independent of the input data is inserted in its place. The result is an approach that can provide stronger privatization on image data, and yet be preserving both the domain and the utility of the inputs.

## 1 INTRODUCTION

The amounts of data required for training machine learning models for the processing of natural language and images are growing with the scale and capabilities of the models (Goodfellow et al., 2016). However, collecting and using large datasets which may contain sensitive information about individuals is often impeded by increasingly strong privacy laws protecting individual rights, and the infeasibility of obtaining individual consent. Giving privacy guarantees on a dataset may let us share data, while protecting the rights of individuals, and thus unlocking the large benefits for individuals and for society that big datasets can provide.

In this work, we study techniques for selective obfuscation of image datasets. These techniques aim to provide the original data as detailed as possible while making it hard for an adversary to detect specific sensitive attributes. The proposed solution is agnostic to the downstream task, with the objective to make the data as private as possible given a distortion constraint.

Previous research has addressed this issue using adversarial representation learning with some success: a filter model is trained to obfuscate sensitive information while an adversary model is trained to recover the information (Edwards & Storkey, 2016). We instead explore this task under the assumption that *it is easier to hide sensitive information if you replace it with something else*: a sample which is independent from the input data.

In our setup, the adversary can make an arbitrary number of queries to the model, each time another sample will be produced from the distribution of the sensitive data, while keeping as much as possible of the non-sensitive information about the requested data point.

Aside from the adversary module, our proposed solution includes two main components: one filter model that is trained to remove the sensitive attribute, and one generator model that inserts a synthetically generated new value for the sensitive attribute. The generated sensitive attribute is entirely independent from the sensitive attribute in the original input image. Following a body of work in privacy-related adversarial learning we evaluate the proposed model on faces from the CelebA dataset (Liu et al., 2015), and consider, for example, the smile or gender of a person to be the sensitive attribute. The smile is an attribute that carries interesting aspects in the transformations of a human face. The obvious change reside close to the mouth when a person smiles, but also other

---

subtle changes occur: eyelids tighten, dimples may show and the skin may wrinkle. The current work includes a thorough analysis of the dataset, including correlations of such features. These correlations make the task interesting and challenging, reflecting the real difficulty that may occur when anonymizing data. What is the right trade-off between preserving the utility as defined by allowing information about other attributes to remain, and removing the sensitive information?

## 2 RELATED WORK

Privacy-preserving machine learning has been studied from a number of different angles. Some of this work has assumed access to a privacy-preserving mechanism, such as bounding boxes for faces, and has studied how to hide people’s identity by blurring (Oh et al., 2016a), removing (Orekondy et al., 2018) or generating the face of other people (Hukkelås et al., 2019) in their place. Other work has assumed access to the utility-preserving mechanism and proposed to obfuscate everything except what they want to retain (Alharbi et al., 2019). This raises the question: how do we find the pixels in an image that need to be modified to preserve privacy with respect to some attribute?

Furthermore, Oh et al. (2016b) showed that blurring or removing the head of a person has a limited effect on privacy. The finding is crucial; *we cannot rely on modifications of an image such as blurring or overpainting to achieve privacy*. An adversarial set-up instead captures the signals that the adversary uses, and can attain a stronger privacy.

Adversarial learning is the process of training a model with the objective of being able to fool an adversary (Goodfellow et al., 2014). Both models are trained simultaneously, and become increasingly good at their respective task during the training process. This approach has been successfully used to learn image-to-image transformations (Isola et al., 2017; Choi et al., 2018), and synthesis of properties such as facial expressions (Song et al., 2017; Tang et al., 2019). Privacy-preserving adversarial representation learning studies how to utilize this learning framework to learn representations of data that hide some sensitive information (Edwards & Storkey, 2016; Zhang et al., 2018; Xie et al., 2017; Beutel et al., 2017; Raval et al., 2017).

Bertran et al. (2019) presented a privacy preserving mechanism that minimizes the mutual information between the utility variable and the input image data conditioned on the learned representation. In Roy & Boddeti (2019), the generator is optimized to maximize the entropy of the discriminator output rather than to minimize the log likelihood, which is beneficial in the multi-class setting. Osia et al. (2020) approached the problem using an information-bottleneck. Wu et al. (2018), Ren et al. (2018), and Wang et al. (2019) studied how to learn transformations of video that respect a privacy budget while maintaining performance on the downstream task. Tran et al. (2018) proposed an approach for pose-invariant face recognition. Similar to our work, their approach used adversarial representation learning to disentangle specific attributes in the data. Oh et al. (2017) trained a model to add a small amount of noise to the input to hide the identity of a person.

All of these, with the exception of Edwards & Storkey (2016) (see below), depend on knowing the downstream task labels. *Our work has no such dependency: the data produced by our method is designed to be usable regardless of downstream task.*

In Edwards & Storkey (2016), a limited artificial experiment is included which does not depend on the downstream task. In the experiment, they remove sensitive text which was overlaid on images, a task which is much simpler than the real-world problem considered in the current work. The overlaid text is independent of the underlying image, and therefore the solution does not require a trade-off between utility and privacy which is the case in most real settings. Furthermore, they assume that it is sufficient to remove the sensitive information, while we also replace the sensitive information with synthetic information which we show further strengthens the privacy. Our approach also allows for choosing a maximum distortion budget.

Like in the current work, Huang et al. (2017, 2018) use adversarial learning to minimize the mutual information between the private attribute and the censored image under a distortion constraint. We extend on these ideas by proposing a modular design consisting of a filter that is adversarially trained to obfuscate the data, and a generator that further enhances the privacy by adding new independently sampled synthetic information for the sensitive attributes.

---

### 3 PRIVACY-PRESERVING ADVERSARIAL REPRESENTATION LEARNING

In the current work, we focus on utility-preserving transformations of data: we use privacy-preserving representation learning to obfuscate information in the input data, and seek to output results that retain the information and structure of the input.

#### 3.1 PROBLEM SETTING

Generative adversarial privacy (GAP) (Huang et al., 2018) was proposed as a method to provide privacy in images under a distortion constraint, and will be used as the baseline in the current work. In GAP, one assumes a joint distribution  $P(X, S)$  of public data points  $X$  and sensitive private attributes  $S$  where  $S$  is typically correlated with  $X$ . The authors define a privacy mechanism  $X' = f(X, Z_1)$  where  $Z_1$  is the source of noise or randomness in  $f$ . Let  $h_f(X')$  be an adversary’s prediction of the sensitive attribute  $S$  from the privatized data  $X'$  according to a decision rule  $h_f$ . The performance of the adversary is thus measured by a loss function  $\ell_f(h_f(f(x, z_1)), s)$  and the expected loss of the adversary with respect to  $X, S$  and  $Z_1$  is

$$L_f(h_f, f) = \mathbb{E}_{\substack{x, s \sim p(x, s) \\ z_1 \sim p(z_1)}}[\ell_f(h_f(f(x, z_1)), s)], \quad (1)$$

where  $p(z_1)$  is the source of noise.

The privacy mechanism  $f$  will be trained to be privacy-preserving and utility-preserving. That is, it should be hard for an analyst to infer  $S$  from  $X'$ , but  $X'$  should be minimally distorted with respect to  $X$ . Huang et al. (2018) formulate this as a constrained minimax problem

$$\min_f \max_{h_f} -L_f(f, h_f) \quad \text{s.t.} \quad \mathbb{E}_{\substack{x, s \sim p(x, s) \\ z_1 \sim p(z_1)}}[d(f(x, z_1), x)] \leq \epsilon_1, \quad (2)$$

where the constant  $\epsilon_1 \geq 0$  defines the allowed distortion for the privatizer and  $d(\cdot, \cdot)$  is some distortion measure.

In the current work,  $f$  will be referred to as the *filter* since the purpose of it is to filter the sensitive information from  $x$ . A potential limitation with this formulation is that it only obfuscates the sensitive information in  $x$  which may make it obvious to the adversary that  $x'$  is a censored version of  $x$ . Instead, we propose to replace the sensitive information with a new independent value  $s'$ .

#### 3.2 OUR CONTRIBUTION

We extend the filter with a *generator* module  $g$ , defined as  $X'' = g(f(X, Z_1), S', Z_2)$  where  $S'$  denotes the random variable of the new synthetic value for the sensitive attribute.  $Z_1$  and  $Z_2$  denote the sources of randomness in  $f$  and  $g$  respectively. The discriminator  $h_g$  is trained to predict  $s$  when the input is a real image, and to predict the “*fake*” output when the input comes from  $g$  as in the learning setup in Salimans et al. (2016). The objective of the generator  $g(x', s', z_2)$  is to generate a new synthetic (independent) sensitive attribute  $s'$  in  $x'$ , that will fool the discriminator  $h_g$ . We define the loss of the discriminator  $h_g$  as

$$L_g(h_g, g) = \mathbb{E}_{\substack{x, s \sim p(x, s) \\ s' \sim p(s') \\ z_1, z_2 \sim p(z_1, z_2)}}[\ell_g(h_g(g(f(x, z_1), s', z_2)), fake)] + \mathbb{E}_{x, s \sim p(x, s)}[\ell_g(h_g(x), s)], \quad (3)$$

where  $p(z_1, z_2)$  is the source of noise,  $p(s')$  is the assumed distribution of the synthetic sensitive attributes  $s'$ , *fake* is the fake class, and  $\ell_g$  is the loss function. We formulate this as a constrained minimax problem

$$\min_g \max_{h_g} -L_g(g, h_g) \quad \text{s.t.} \quad \mathbb{E}_{\substack{x, s \sim p(x, s) \\ s' \sim p(s') \\ z_1, z_2 \sim p(z_1, z_2)}}[d(g(f(x, z_1), s', z_2), x)] \leq \epsilon_2, \quad (4)$$

where the constant  $\epsilon_2 \geq 0$  defines the allowed distortion for the generator.

### 3.3 IMPLEMENTATION

Let  $\mathcal{D} = \{(x_i, s_i)\}_{i=1}^n$  be a dataset of samples  $(x_i, s_i)$  which are assumed to be identically and independently distributed according to some unknown joint distribution  $P(X, S)$ . We assume that the sensitive attribute is binary and takes values in  $\{0, 1\}$ . However, the proposed approach can easily be extended to categorical sensitive attributes.  $g(X', S', Z_2; \theta_g)$  using convolutional neural networks of the UNet (Ronneberger et al., 2015) architecture parameterized by  $\theta_f$  and  $\theta_g$ , respectively. (See Appendix A.1 for details).

The discriminators  $h_f(X'; \phi_f)$  and  $h_g(X''; \phi_g)$  are modeled using ResNet-18 (He et al., 2016) and a modified version which we refer to as ResNet-10<sup>1</sup>, respectively. The last fully connected layer has been replaced with a two and three class output layer for each model, respectively.

As suggested by Roy & Boddeti (2019), we choose the filter discriminator loss  $\ell_f$  to be the negative entropy. Intuitively, this leads to  $f$  learning to make the adversary  $h_f$  confused about the sensitive attribute rather than to make it certain of the wrong value. For completeness, we also include experiments where  $\ell_f$  is the categorical cross-entropy, as are  $\ell_{h_f}$  and  $\ell_g$ . The distortion measure  $d$  is defined as the  $L_2$ -norm, and  $p(s')$  is assumed to be the uniform distribution  $\mathcal{U}\{0, 1\}$ . The hyperparameters consist of the learning rate  $lr$ , the quadratic penalty term coefficient  $\lambda$ , the distortion constraint  $\epsilon$ , and the  $(\beta_1, \beta_2)$  parameters to Adam (Kingma & Ba, 2014). Details of the training setup can be found in Appendix A.3, and the full code is published on GitHub<sup>2</sup>.

## 4 EXPERIMENTS

In this section we describe our experiments, the dataset used to evaluate the method and the evaluation metrics. We evaluate our method on the facial images from the CelebA dataset (Liu et al., 2015)<sup>3</sup>.

### 4.1 CELEBA

The CelebA dataset Liu et al. (2015) consists of 202,599 face images of size 218x178 pixels and 40 binary attribute annotations per image, such as age (old or young), gender, if the image is blurry, if the person is bald, etc. The dataset has an official split into a training set of 162,770 images, a validation set of 19,867 images and a test set of 19,962 images. We resize all images to 64x64 for the quantitative experiments, and to 128x128 pixels for the qualitative experiments, and normalize all pixel values to the region  $[0, 1]$ . We use a higher resolution for the qualitative results to make subtle visual changes more apparent.

### 4.2 FILTERING AND REPLACEMENT OF SENSITIVE DATA

Let  $\mathcal{D}_{train} = \{(x_i, s_i)\}_{i=1}^n$  be a set of training data where  $x_i$  denotes facial image  $i$  and  $s_i \in \{0, 1\}$  denotes the sensitive attribute. Further let  $\mathcal{D}_{test} = \{(x_i, s_i)\}_{i=1}^m$  be the held out test data. For the purpose of evaluation, we assume access to a number of utility attributes  $u^{(j)} \in \{0, 1\}$  for each  $x$  and  $j \in U$ . The following attributes provided with the dataset will be used in the experiments: *gender*, *lipstick*, *age*, *high cheekbones*, *mouth slightly open*, *heavy makeup*, *smiling*. In each experiment, one of these will be selected as the sensitive attribute, and the rest will be considered the utility attributes. The utility attributes are not used during training, but it allows for a utility score in the evaluation. The utility attributes are used to evaluate how well non-sensitive attributes are preserved after the images have been censored. We compute an average over fixed classifiers, trained to predict each respective utility attribute on the original training data, when evaluated on the censored data.

We train the models using  $\mathcal{D}_{train}$  with  $lr = 0.0005$ ,  $\lambda = 10^5$ ,  $\epsilon \in \{0.03, 0.02, 0.01, 0.005, 0.001\}$ , and  $(\beta_1, \beta_2) = (0.9, 0.999)$ . We define the training data censored by the filter as  $\mathcal{D}'_{train} = \{(x'_i, s_i)\}_{i=1}^n$ , where  $x'_i = f(x_i, z_i^{(1)}; \theta_f)$  and the training data censored by the filter and the generator

<sup>1</sup>ResNet-10 has the same setup as ResNet-18, but each of the “conv2\_x”, “conv3\_x”, “conv4\_x”, and “conv5\_x” layers consists of only one block instead of two.

<sup>2</sup><https://github.com/anonymouse/anonymouse-repo-name>

<sup>3</sup><http://mmlab.ie.cuhk.edu.hk/projects/CelebA.html>

as  $\mathcal{D}'_{train} = \{(x''_i, s_i)\}$  where  $x''_i = g(x'_i, s'_i, z_i^{(2)}; \theta_g)$ ,  $z_i^{(1)}, z_i^{(2)} \sim \mathcal{N}(\mathbf{0}, \mathbf{1})$ , and  $s'_i \sim \mathcal{U}\{0, 1\}$ . We do the same transformations to the test data and denote them  $\mathcal{D}'_{test}$  and  $\mathcal{D}''_{test}$  respectively.

Each experiment was performed on a Tesla V100 SXM2 32 GB in a DGX-1 machine. The training was restricted to 100 epochs which takes about 13 hours. We run each experiment with negative entropy loss three times, and present the average over these runs, and we run each experiment with log-likelihood loss five times and present the average over these.

### 4.3 EVALUATION

To evaluate the privacy loss for each method we train an adversarial classifier to predict the ground truth sensitive attribute given a training set of images censored by each privatization method, and then we evaluate each adversary on a test set of censored images. If an adversary can predict the ground truth sensitive attribute of censored images, that it has not seen before, with high accuracy, then the privacy loss is high. Let  $adv(s|\cdot)$  denote an adversary trained on the censored training set to predict the ground truth attribute  $s$ , then the privacy loss is defined as

$$Privacy\ loss = \frac{1}{|\mathcal{D}_{test}|} \sum_{(x,s) \in \mathcal{D}_{test}} \mathbb{1}[adv(s|g(f(x), s')) = s]. \quad (5)$$

To evaluate the utility score for each method, we use fixed classifiers that have been pre-trained on the original data to predict a set of utility attributes that are considered non-sensitive. If these utility attributes are predictable with high accuracy after privatization of the image, then we consider the method to have a high utility score. Let  $fix(u|\cdot)$  denote a fixed classifier trained on the original training set to predict the ground truth attribute  $u$ , then the utility score is defined as

$$Utility\ score = \frac{1}{|U|} \sum_{j \in U} \frac{1}{|\mathcal{D}_{test}|} \sum_{(x, u^{(j)}) \in \mathcal{D}_{test}} \mathbb{1}[fix(u|g(f(x), s')) = u^{(j)}]. \quad (6)$$

We then plot the utility score against the privacy loss for different distortion budgets and get a trade-off curve. Similar evaluation method are used in Roy & Boddeti (2019); Bertran et al. (2019). In particular, Roy & Boddeti (2019) plot accuracy of an adversary predicting the sensitive attribute against the accuracy of a classifier predicting the target attribute.

## 5 RESULTS

In this section we present quantitative and qualitative results on the facial image experiments.

### 5.1 QUANTITATIVE RESULTS

Figure 1 shows the trade-off between privacy loss and utility score when evaluated on censored images. Our method consistently has a higher utility at any given level of privacy compared to the baseline. Remember: these are strong adversaries required to run tagged training data through the privacy mechanism to be able to train. Additional results can be found in Appendix A.2.

To further show that explicitly optimizing for privacy in the privatization mechanism is necessary we have conducted a similar experiment using StarGAN Choi et al. (2018) to randomly change the sensitive attribute in the image (results in suppl.). We then evaluate the censored images, which look very convincing to a human, using adversarial classifiers. The adversaries can successfully detect the sensitive attributes with an accuracy of roughly 90%. For the weight  $\lambda_{rec}$  of the cycle consistency loss we explored values  $\{0, 5, 10, 50\}$ . We obtain similar scores when we exclude the filter part of our method and use only the generator part to censor the images (see Appendix A.2).

In Table 1 we present the results of evaluating the accuracy of  $fix(s|\cdot)$  on the dataset  $\{x''_i, s'_i\}_{i=1}^m$  where  $x''_i = g(x'_i, s'_i, z_i^{(2)})$  is the image censored with our method and  $s'_i$  is the new synthetic attribute uniformly sampled from  $\{0, 1\}$ . That is, we measure how often the classifier predict the new synthetic attribute  $s'_i$  when applied to  $x''_i$ . We can see that with  $\epsilon = 0.001$  the method is on average able to fool the classifier 82.4% of the time for the *smiling* attribute, and this increases with larger distortion

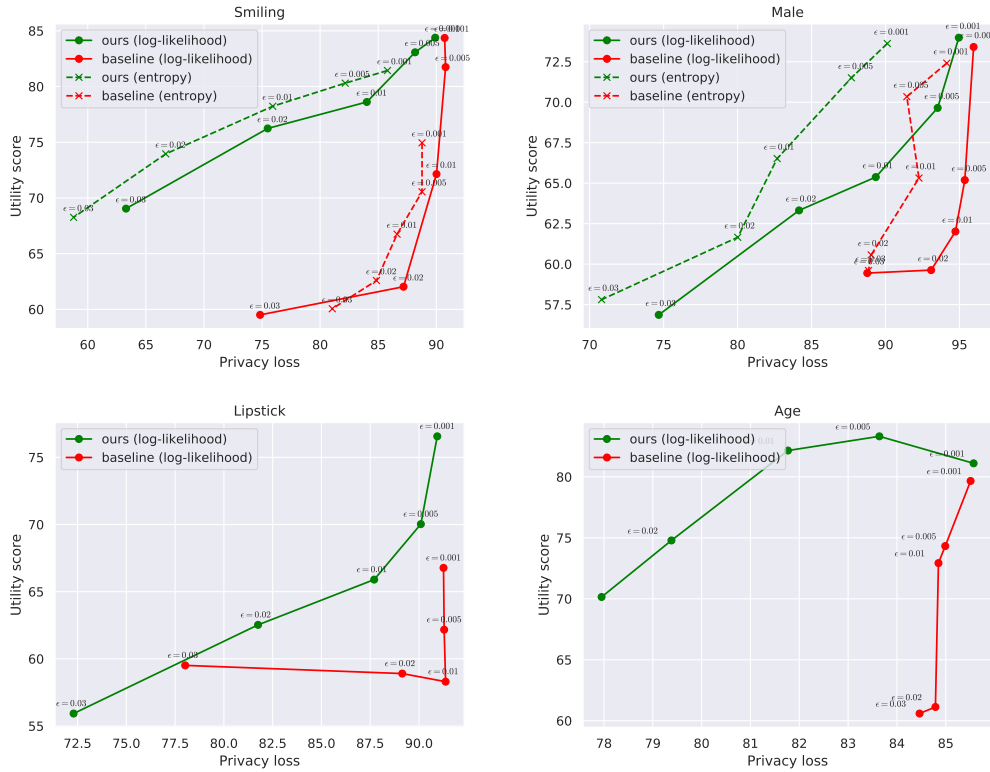


Figure 1: Privacy vs. utility trade-off curve where the sensitive attribute is *smiling* (top left), *gender* (top right), *lipstick* (bottom left), *age* (bottom right). Our approach with negative entropy loss consistently outperforms all other approaches on the attributes explored, and our method with log-likelihood loss outperforms the baseline with log-likelihood loss on all explored attributes.

Table 1: The success rate of our method to fool a fixed classifier for the sensitive attributes *smiling*, *gender*, *lipstick*, and *age*. This was measured as the accuracy of  $fix(s|\cdot)$  for each censored attribute in the censored data  $\{(x_i'', s_i')\}_{i=1}^m$ . Higher is better. Average and standard deviation of five runs.

Dist. $\epsilon$	Synthetic			
	Smiling	Gender	Lipstick	Young
0.001	$82.4 \pm 2.1$	$72.9 \pm 1.5$	$62.2 \pm 3.1$	$59.2 \pm 1.9$
0.005	$86.4 \pm 3.7$	$79.4 \pm 0.6$	$71.7 \pm 2.4$	$62.1 \pm 2.5$
0.01	$87.4 \pm 2.1$	$85.6 \pm 1.4$	$77.6 \pm 2.4$	$59.6 \pm 1.6$
0.05	$91.2 \pm 2.9$	$90.3 \pm 4.3$	$90.6 \pm 4.2$	$67.7 \pm 2.1$

budget  $\epsilon$  to a success rate of 91.2% on average with  $\epsilon = 0.05$ . The results are similar when the images have been censored with respect to the attributes *gender*, *lipstick*, and *age*, but these require a larger distortion budget.

Table 2 shows the correlations between classifier predictions on a pair of attributes when one attribute has been synthetically replaced.

## 5.2 QUALITATIVE RESULTS

Figure 2 shows, from the top row to the bottom row, the input image  $x$ , the censored image  $x'$ , the censored image  $x''$  with the synthetic attribute  $s' = 0$  (non-smiling), and the censored image  $x''$  with

Table 2: The value of each cell denotes the Pearson’s correlation coefficient between predictions from a classifier trained to predict the row attribute and a classifier trained to predict the column attribute, given that the column attribute has been censored.

	Smiling	Gender	Lipstick	Young
Smiling	1.00	-0.04	0.08	-0.06
Gender	-0.07	1.00	-0.44	-0.21
Lipstick	0.14	-0.30	1.00	0.26
Young	0.05	-0.11	0.23	1.00
High Cheekbones	0.14	-0.07	0.15	-0.01
Mouth Open	0.04	0.00	0.03	-0.02
Heavy Makeup	0.12	-0.24	0.47	0.22

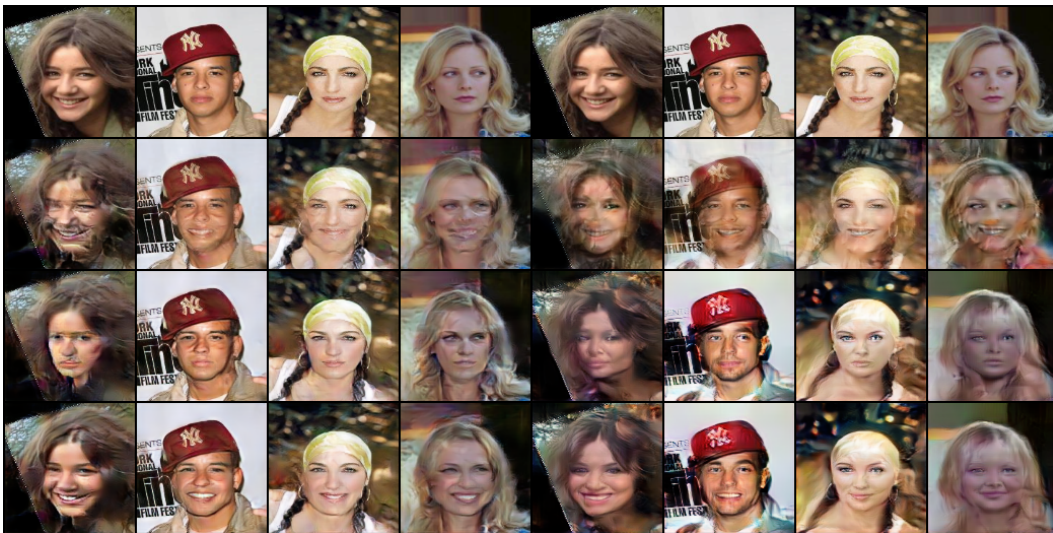


Figure 2: Qualitative results for the sensitive attribute smile. In the first four columns:  $\epsilon = 0.001$ , and in the last four columns:  $\epsilon = 0.01$ . From top to bottom row: input image ( $x$ ), censored image ( $x'$ ), censored image with synthetic non-smile ( $x''$ ,  $s' = 0$ ), censored image with synthetic smile ( $x''$ ,  $s' = 1$ ). The model is able to generate a synthetic smiling attribute while maintaining much of the structure in the image. These images were generated from a model trained using 128x128 pixels.

the synthetic attribute  $s' = 1$  (smiling). A value of  $\epsilon = 0.001$  is used in the first four columns, and  $\epsilon = 0.01$  in the last four columns. The images censored by our method look sharper and it is less obvious that they are censored. We can see that the method convincingly generates non-smiling faces and smiling faces while most of the other parts of the image is intact. These images are sampled from models trained on images of 128x128 pixels resolution. See Figure 4 in Appendix A.2 for corresponding samples on the same input images, but using *gender* as the sensitive attribute.

## 6 DISCUSSION

Our method consistently outperforms the baseline, ensuring a higher level of privacy while maintaining more of the useful information (see Figure 1). For all sensitive attributes that we consider and at nearly all given distortion budgets ( $\epsilon \in \{0.02, 0.01, 0.005, 0.001\}$ ) we observe both a higher privacy and a higher utility for our method. At extreme distortions ( $\epsilon = 0.03$ ) we still observe high privacy but also a lower utility score for some of the attributes. Furthermore, we can observe that using the entropy loss function for the filter benefits both the baseline and our method. We only

---

explored the negative entropy loss for the *smiling* and *male* attributes due to compute limitations, but expect similar results for other attributes.

This shows that our method makes it more difficult for the adversary to see through the privatization step at each given distortion budget. To show the effect of the filter we have conducted experiments where we only use the generator to privatize the images (see Appendix A.2), which does not seem to provide any privacy.

A possible problem when using the generator without the filter is that the generator could learn the following rule: if the sensitive attribute in the image that is being censored is the same as the randomly sampled attribute, let the image through without changes. Otherwise, apply the  $\epsilon$ -constrained change that transforms the image into a realistic image with the new attribute. If the transformed image is indistinguishable from a real image this is not a problem, but if it is not we can easily reverse the privatization by detecting if the image is real or not. The filter step mitigates this by *always* removing the sensitive data in the image, forcing the generator to synthesize new data. Since the censored image is now guaranteed to be synthetic, we can no longer do the simple real/fake attack.

Similarly, we conduct experiments where we use StarGAN to censor the images, but observe no privacy when using this standard attribute manipulation method. A reason could be that the cyclic consistency loss term actually encourage image transformations that are easily invertible given the original attribute, which is not desirable in a privacy setting. This motivates our approach which is explicit about the privacy objective.

In Table 1, we see that the fixed smile classifier is fooled by our privatization mechanism in 82.4% to 91.2% of the data points in the test set (depending on the distortion  $\epsilon$ ). These results indicate that it may be harder for an adversarially trained classifier to predict the sensitive attribute when it has been replaced with something else, as compared to simply removed. We assume that this is due to the added variability in the data. Or intuitively: it is easier to “blend in” with other images that have similar demonstrations of smiles.

The fact that many important attributes in facial images correlate leads to the reflection that disentangling the underlying factors of variation is not entirely possible. For example, in this dataset lipstick is highly correlated with female gender. This means that if we want to hide all information about whether or not the person is wearing lipstick we also need to hide its gender (and other correlating attributes). This problem can be seen in Table 2 where changing whether or not a person is wearing lipstick correlates with changes of gender.

The question is: if we censor an attribute in an image, how does that correlate with changes of other attributes in the image? In the lipstick column of Table 2 we have censored the attribute lipstick. We then make predictions on whether or not the person in the censored image is wearing lipstick, and compute the correlation between these predictions and predictions for the attributes for each row. We can see that changes in lipstick correlate negatively with changes in gender and positively with makeup. This highlights the problem of disentangling these underlying factors of variation.

A strength of our method is that it is *domain-preserving*, this allows a utility provider to use the censored image in existing algorithms without modifications. Since the method also preserves utility this may also allow stacking the privatization mechanism to censor multiple attributes in an image.

## 7 CONCLUSIONS

In this work we have presented a strong privacy-preserving transformation mechanism for image data which is learned using an adversarial setup. While previous work on adversarial representation learning has focused on removing information from a representation, our approach extends on this and can also generate new information in its place that looks realistic and gives further privacy properties compared to the baseline. We evaluate our method using adversarially trained classifiers, and our results show that not only do we provide stronger privacy with regards to sensitive attributes, but we also preserve non-sensitive attributes of the image at a higher rate. The results show that the synthetically added attribute gives stronger privacy properties and helps fooling the adversary in the challenging setting where the adversary is allowed to be trained using the output of the privacy mechanism.



---

## REFERENCES

- Rawan Alharbi, Mariam Tolba, Lucia C. Petitto, Josiah Hester, and Nabil Alshurafa. To mask or not to mask? balancing privacy with visual confirmation utility in activity-oriented wearable cameras. *Proc. ACM Interact. Mob. Wearable Ubiquitous Technol.*, 3(3), September 2019. doi: 10.1145/3351230. URL <https://doi.org/10.1145/3351230>.
- Martin Bertran, Natalia Martinez, Afroditi Papadaki, Qiang Qiu, Miguel Rodrigues, Galen Reeves, and Guillermo Sapiro. Adversarially learned representations for information obfuscation and inference. In Kamalika Chaudhuri and Ruslan Salakhutdinov (eds.), *Proceedings of the 36th International Conference on Machine Learning*, volume 97 of *Proceedings of Machine Learning Research*, pp. 614–623, Long Beach, California, USA, 09–15 Jun 2019. PMLR.
- Alex Beutel, Jilin Chen, Zhe Zhao, and Ed H Chi. Data decisions and theoretical implications when adversarially learning fair representations. *arXiv preprint arXiv:1707.00075*, 2017.
- Yunjey Choi, Minje Choi, Munyoung Kim, Jung Woo Ha, Sunghun Kim, and Jaegul Choo. StarGAN: Unified Generative Adversarial Networks for Multi-domain Image-to-Image Translation. *Proceedings of the IEEE Computer Society Conference on Computer Vision and Pattern Recognition*, pp. 8789–8797, 2018. ISSN 10636919. doi: 10.1109/CVPR.2018.00916.
- Harrison Edwards and Amos J. Storkey. Censoring representations with an adversary. In *4th International Conference on Learning Representations, ICLR 2016, San Juan, Puerto Rico, May 2-4, 2016, Conference Track Proceedings*, 2016.
- Ian Goodfellow, Jean Pouget-Abadie, Mehdi Mirza, Bing Xu, David Warde-Farley, Sherjil Ozair, Aaron Courville, and Yoshua Bengio. Generative adversarial nets. In *Advances in neural information processing systems*, pp. 2672–2680, 2014.
- Ian Goodfellow, Yoshua Bengio, and Aaron Courville. *Deep learning*. MIT press, 2016.
- K. He, X. Zhang, S. Ren, and J. Sun. Deep residual learning for image recognition. In *2016 IEEE Conference on Computer Vision and Pattern Recognition (CVPR)*, pp. 770–778, June 2016. doi: 10.1109/CVPR.2016.90.
- C. Huang, P. Kairouz, and L. Sankar. Generative adversarial privacy: A data-driven approach to information-theoretic privacy. In *2018 52nd Asilomar Conference on Signals, Systems, and Computers*, pp. 2162–2166, Oct 2018. doi: 10.1109/ACSSC.2018.8645532.
- Chong Huang, Peter Kairouz, Xiao Chen, Lalitha Sankar, and Ram Rajagopal. Context-aware generative adversarial privacy. *Entropy*, 19(12), 2017. ISSN 1099-4300. doi: 10.3390/e19120656. URL <https://www.mdpi.com/1099-4300/19/12/656>.
- Håkon Hukkelås, Rudolf Mester, and Frank Lindseth. Deepprivacy: A generative adversarial network for face anonymization. In George Bebis, Richard Boyle, Bahram Parvin, Darko Koracin, Daniela Ushizima, Sek Chai, Shinjiro Sueda, Xin Lin, Aidong Lu, Daniel Thalmann, Chaoli Wang, and Panpan Xu (eds.), *Advances in Visual Computing*, pp. 565–578, Cham, 2019. Springer International Publishing. ISBN 978-3-030-33720-9.
- P. Isola, J. Zhu, T. Zhou, and A. A. Efros. Image-to-image translation with conditional adversarial networks. In *2017 IEEE Conference on Computer Vision and Pattern Recognition (CVPR)*, pp. 5967–5976, July 2017. doi: 10.1109/CVPR.2017.632.
- Diederik P. Kingma and Jimmy Ba. Adam: A method for stochastic optimization, 2014. URL <http://arxiv.org/abs/1412.6980>. cite arxiv:1412.6980Comment: Published as a conference paper at the 3rd International Conference for Learning Representations, San Diego, 2015.
- Ziwei Liu, Ping Luo, Xiaogang Wang, and Xiaoou Tang. Deep learning face attributes in the wild. In *Proceedings of International Conference on Computer Vision (ICCV)*, December 2015.
- Seong Joon Oh, Rodrigo Benenson, Mario Fritz, and Bernt Schiele. Faceless person recognition: Privacy implications in social media. In Bastian Leibe, Jiri Matas, Nicu Sebe, and Max Welling (eds.), *Computer Vision – ECCV 2016*, pp. 19–35, Cham, 2016a. Springer International Publishing. ISBN 978-3-319-46487-9.

- 
- Seong Joon Oh, Rodrigo Benenson, Mario Fritz, and Bernt Schiele. Faceless person recognition: Privacy implications in social media. In *European Conference on Computer Vision*, pp. 19–35. Springer, 2016b.
- Seong Joon Oh, Mario Fritz, and Bernt Schiele. Adversarial image perturbation for privacy protection a game theory perspective. In *2017 IEEE International Conference on Computer Vision (ICCV)*, pp. 1491–1500. IEEE, 2017.
- Tribhuvanesh Orekondy, Mario Fritz, and Bernt Schiele. Connecting pixels to privacy and utility: Automatic redaction of private information in images. In *The IEEE Conference on Computer Vision and Pattern Recognition (CVPR)*, June 2018.
- S. A. Osia, A. Taheri, A. S. Shamsabadi, K. Katevas, H. Haddadi, and H. R. Rabiee. Deep private-feature extraction. *IEEE Transactions on Knowledge and Data Engineering*, 32(1):54–66, Jan 2020. ISSN 2326-3865. doi: 10.1109/TKDE.2018.2878698.
- Nisarg Raval, Ashwin Machanavajjhala, and Landon P Cox. Protecting visual secrets using adversarial nets. In *2017 IEEE Conference on Computer Vision and Pattern Recognition Workshops (CVPRW)*, pp. 1329–1332. IEEE, 2017.
- Zhongzheng Ren, Yong Jae Lee, and Michael S. Ryoo. Learning to anonymize faces for privacy preserving action detection. In Vittorio Ferrari, Martial Hebert, Cristian Sminchisescu, and Yair Weiss (eds.), *Computer Vision – ECCV 2018*, pp. 639–655, Cham, 2018. Springer International Publishing. ISBN 978-3-030-01246-5.
- O. Ronneberger, P.Fischer, and T. Brox. U-net: Convolutional networks for biomedical image segmentation. In *Medical Image Computing and Computer-Assisted Intervention (MICCAI)*, volume 9351 of *LNCS*, pp. 234–241. Springer, 2015. (available on arXiv:1505.04597 [cs.CV]).
- Proteek C. Roy and Vishnu N. Boddeti. Mitigating information leakage in image representations: A maximum entropy approach. In *The IEEE Conference on Computer Vision and Pattern Recognition (CVPR)*, June 2019.
- Tim Salimans, Ian Goodfellow, Wojciech Zaremba, Vicki Cheung, Alec Radford, Xi Chen, and Xi Chen. Improved techniques for training gans. In D. D. Lee, M. Sugiyama, U. V. Luxburg, I. Guyon, and R. Garnett (eds.), *Advances in Neural Information Processing Systems 29*, pp. 2234–2242. Curran Associates, Inc., 2016.
- Lingxiao Song, Zhihe Lu, Ran He, Zhenan Sun, and Tieniu Tan. Geometry guided adversarial facial expression synthesis. *CoRR*, abs/1712.03474, 2017. URL <http://arxiv.org/abs/1712.03474>.
- Hao Tang, Dan Xu, Gaowen Liu, Wei Wang, Nicu Sebe, and Yan Yan. Cycle in cycle generative adversarial networks for keypoint-guided image generation. In *Proceedings of the 27th ACM International Conference on Multimedia*, MM ’19, pp. 2052–2060, New York, NY, USA, 2019. Association for Computing Machinery. ISBN 9781450368896. doi: 10.1145/3343031.3350980. URL <https://doi.org/10.1145/3343031.3350980>.
- Luan Quoc Tran, Xi Yin, and Xiaoming Liu. Representation learning by rotating your faces. *IEEE transactions on pattern analysis and machine intelligence*, 2018.
- Haotao Wang, Zhenyu Wu, Zhangyang Wang, Zhaowen Wang, and Hailin Jin. Privacy-preserving deep visual recognition: An adversarial learning framework and A new dataset. *CoRR*, abs/1906.05675, 2019. URL <http://arxiv.org/abs/1906.05675>.
- Zhenyu Wu, Zhangyang Wang, Zhaowen Wang, and Hailin Jin. Towards privacy-preserving visual recognition via adversarial training: A pilot study. In Vittorio Ferrari, Martial Hebert, Cristian Sminchisescu, and Yair Weiss (eds.), *Computer Vision – ECCV 2018*, pp. 627–645, Cham, 2018. Springer International Publishing. ISBN 978-3-030-01270-0.
- Qizhe Xie, Zihang Dai, Yulun Du, Eduard Hovy, and Graham Neubig. Controllable invariance through adversarial feature learning. In *Advances in Neural Information Processing Systems*, pp. 585–596, 2017.

---

Brian Hu Zhang, Blake Lemoine, and Margaret Mitchell. Mitigating unwanted biases with adversarial learning. In *Proceedings of the 2018 AAAI/ACM Conference on AI, Ethics, and Society*, pp. 335–340. ACM, 2018.

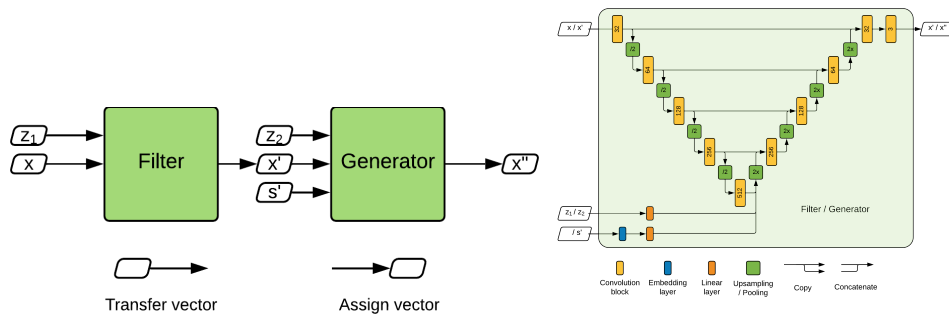


Figure 3: Overview of the training setup (left) and the network architecture used in the filter and the generator (right).

## A APPENDIX

### A.1 ADDITIONAL DETAILS

An overview of the setup can be seen in Figure 3. We use the UNet Ronneberger et al. (2015), illustrated on the right in Figure 3, architecture for both the filter and the generator. The orange blocks are convolution blocks each of which, except for the last block, consist of a convolution layer, a batch normalization layer and a rectified linear activation unit, repeated twice in that order. The number of output channels of the convolution layers in each block has been noted in the figure. The last convolution block with a 3 channel output (the RGB image) consists of only a single convolutional layer followed by a sigmoid activation. The green blocks denote either a max pooling layer with a kernel size of two and a stride of two if marked with “/2” or a nearest neighbor upsampling by a factor of two if marked with “2x”. The blue block denotes an embedding layer, which takes as input the categorical value of the sensitive attribute and outputs a dense embedding of 128 dimensions. It is then followed by a linear projection and a reshaping to match the spatial dimensions of the output of the convolution block to which it is concatenated, but with a single channel. The same type of linear projection is applied on the 1024 dimensional noise vector input, but this projection and reshaping matches both the spatial and channel dimensions of the output of the convolutional block to which it is concatenated. Concatenation is in both cases done along the channel dimension.

### A.2 ADDITIONAL RESULTS

The results in Table 3 show that using the filter together with the generator ( $g \circ f$ ) give a stronger privatization guarantee than using only the generator (without the filter) or only the baseline (the filter without the generator).

Table 3: The results of evaluating the adversarially trained classifiers  $adv(s|\cdot)$  on the held out test data censored with the baseline, only the generator, and our method for varying distortion  $\epsilon$  for the *smiling* attribute. Closer to 50 means more privacy. Only using the generator does not provide any privacy, but using it together with the filter provides the best privacy. Lower is better.

Dist. $\epsilon$	Adversarial smiling		
	baseline ( $f$ )	generator ( $g$ )	ours ( $g \circ f$ )
0.001	89.3	90.7	88.7
0.005	89.9	91.2	85.9
0.01	89.8	91.5	83.2
0.05	69.2	78.7	54.1

In Figure 4 we show additional qualitative results when the attribute *gender* is considered sensitive.



Figure 4: Qualitative results for the sensitive attribute gender. In the first four columns:  $\epsilon = 0.001$ , and in the last four columns:  $\epsilon = 0.01$ . From top to bottom row: input image ( $x$ ), censored image ( $x'$ ), censored image with synthetic female gender ( $x''$ ,  $s' = 0$ ), censored image with synthetic male gender ( $x''$ ,  $s' = 1$ ). The model is able to generate a synthetic gender while maintaining much of the structure in the image. These images were generated from a model trained using 128x128 pixels.

### A.3 TRAINING SETUP

Algorithm 1 demonstrates the training setup for our method. Note that when  $\ell_f$  is negative entropy it does not depend on the  $1 - s_i$  argument, but is simply computed from the output of the discriminator  $h_f$ . However, when  $\ell_f$  is cross entropy we optimize the filter such that the discriminator  $h_f$  is fooled into predicting the complement class  $1 - s$ . This means that we need to assume  $s$  to be a binary attribute when using this loss. When using the negative entropy we do not need to make this assumption, which is a strength of the proposed method.

---

**Algorithm 1**

---

**input:**  $\mathcal{D}, lr, \lambda, \epsilon, \beta_1, \beta_2$

$\epsilon_1, \epsilon_2 \leftarrow \epsilon$

**repeat**

Draw  $m$  samples uniformly at random from the dataset

$(x_1, s_1), \dots, (x_m, s_m) \sim \mathcal{D}$

Draw  $m$  samples from the noise distribution

$(z_1^{(1)}, z_1^{(2)}), \dots, (z_m^{(1)}, z_m^{(2)}) \sim p(z^{(1)}, z^{(2)})$

Draw  $m$  samples from the synthetic distribution

$s'_1, \dots, s'_m \sim p(s')$

Compute censored and synthetic data

$x'_1, \dots, x'_m = f_{\theta_f}(x_1, z_1^{(1)}), \dots, f_{\theta_f}(x_m, z_m^{(1)})$

$x''_1, \dots, x''_m = g_{\theta_g}(x'_1, s'_1, z_1^{(2)}), \dots, g_{\theta_g}(x'_m, s'_m, z_m^{(2)})$

Compute filter and generator losses

$$\Theta_f(\theta_f) = \frac{1}{m} \sum_{i=1}^m \ell_f(h_f(x'_i; \phi_f), 1 - s_i) \\ + \lambda \max\left(\frac{1}{m} \sum_{i=1}^m d(x'_i, x_i) - \epsilon, 0\right)^2$$

$$\Theta_g(\theta_g) = \frac{1}{m} \sum_{i=1}^m \ell_g(h_g(x''_i; \phi_g), s'_i) \\ + \lambda \max\left(\frac{1}{m} \sum_{i=1}^m d(x''_i, x_i) - \epsilon, 0\right)^2$$

Update filter and generator parameters

$\theta_f \leftarrow \text{Adam}(\Theta_f(\theta_f); lr, \beta_1, \beta_2)$

$\theta_g \leftarrow \text{Adam}(\Theta_g(\theta_g); lr, \beta_1, \beta_2)$

Compute discriminator losses

$\Phi_f(\phi_f) = \frac{1}{m} \sum_{i=1}^m \ell_{h_f}(h_f(x'_i; \phi_f), s_i)$

$\Phi_g(\phi_g) = \frac{1}{m} \sum_{i=1}^m \ell_g(h_g(x''_i; \phi_g), \text{fake})$

$$+ \frac{1}{m} \sum_{i=1}^m \ell_g(h_g(x_i; \phi_g), s_i)$$

Update discriminator parameters

$\phi_f \leftarrow \text{Adam}(\Phi_f(\phi_f); lr, \beta_1, \beta_2)$

$\phi_g \leftarrow \text{Adam}(\Phi_g(\phi_g); lr, \beta_1, \beta_2)$

**until** stopping criterion

**return**  $\theta_f, \theta_g, \phi_f, \phi_g$

---